Available online at www.sciencedirect.com
SCIENCE DIRECT
Carbohydrate Polymers 64 (2006) 560–568
Carbohydrate Polymers
www.elsevier.com/locate/carbpol

Preparation and characterization of polyaniline/chitosan blend film

Tuspon Thanpitcha [a], Anuvat Sirivat [a], Alexander M. Jamieson [b], Ratana Rujiravanit [a,*]

[a] *Conductive and Electroactive Polymers Research Unit, The Petroleum and Petrochemical College, Chulalongkorn University, Bangkok 10330, Thailand*
[b] *Department of Macromolecular Science, Case Western Reserve University, Cleveland, OH, USA*

Received 20 June 2005
Available online 25 January 2006

Abstract

Films consisting of a blend of a chitosan hydrogel and a conductive polymer, polyaniline (PANI), were prepared and characterized for their electrical and mechanical properties. Polyaniline in emeraldine base (EB) form was dispersed in chitosan solution and blend films were obtained by solution casting. The PANI particles in the blend films were then doped with HCl where we observed reductions in the film tensile strength and Young's modulus by about 30%, but the films electrical conductivity increased by 6 orders of magnitude. The highest electrical conductivity of the blend films was of the order 10^{-4} S/cm. The electrical and mechanical properties of the films varied with polyaniline content, acid dopant type, acid dopant concentration, and doping time.

Keywords: Blend film; Conductive polymer; Hydrogel; Polyaniline; Chitosan

1. Introduction

Polyaniline (PANI) is one of the most extensively studied conductive polymers. Potential applications include uses in rechargeable batteries, sensors, switchable membranes, anticorrosive coatings, and electronic devices (Cho, Park, Hwang, & Choi, 2004). Polyaniline is commercially attractive owing to its easy synthesis either through chemical or electrochemical methods, good environmental stability, ease of conductivity control, and inexpensive production in large quantities. However, like other conductive polymers, polyaniline by itself cannot be easily fabricated as a thin film form with good mechanical properties. Thus, its practical use has been limited.

A number of attempts have been made to fabricate polyaniline blends and composites with improved processibility and mechanical properties while retaining the inherent conductivity of the polymer. Polyaniline blends can be prepared by blending polyaniline with other polymers in solution or in the melt state. Alternatively, aniline can be polymerized chemically or electrochemically in a solution of a matrix polymer. Polymers that have been used to prepare conductive polyaniline blends include epoxy resin (Yang, Zhao, Yu, & Wei, 2004), polyethylene (Chipara *et al.*, 2003), poly(vinyl alcohol) (Gangopadhyay, De, & Ghosh, 2001; Mirmohseni & Wallace, 2003; Zhang & Wan, 2002), polystyrene (Gupta, Singh, & Dubey, 2004), poly(acrylic acid) (Lima Pacheco, Araujo, & de Azevedo 2003), and poly(vinyl chloride) (Gupta & Singh, 2004). Recently, blends consisting of a conductive polymer and a hydrogel have received attention because they can form electroactive hydrogels that are capable of undergoing chemical and/or physical transitions in response to an electrical potential. Therefore, the integration of these two types of materials has been investigated for application in biosensors (Brahim, Narinesingh, & Guiseppi-Elie, 2002) and controlled drug release (Small, Too, & Wallace, 1997). Examples of conductive polymer/hydrogel blends are polypyrrole/poly(2-hydroxyethyl metharylate) (Brahim, Narinesingh, & Guiseppi-Elie, 2002), polypyrrole/polyacrylamide (Small, Too, & Wallace, 1997), and polypyrrole/polyacrylic acid (Kim, Spinks, Too, Wallace, & Bae, 2000).

Chitosan, a copolymer of β[1,4]-linked 2-acetamido-2-deoxy-D-glucopyranose and 2-amino-2-deoxy-D-glucopyranose, is generally obtained by deacetylation of chitin, which is the main component of the exoskeleton of crustacean shells, such as shrimps. This polymer possesses hydrogel-like properties through a reaction with glutaraldehyde as a crosslinking agent. In the form of a hydrogel,

* Corresponding author. Tel.: +66 2 218 4131; fax: +66 2 611 7221.
E-mail address: ratana.r@chula.ac.th (R. Rujiravanit).

0144-8617/$ - see front matter © 2005 Elsevier Ltd. All rights reserved.
doi:10.1016/j.carbpol.2005.11.026

chitosan is used in a wide range of applications such as wastewater treatment (Crini, 2005), separation membrane (Won, Feng, & Lawless 2002), food packaging (Arvanitoyannis, Kulokuris, Nakayama, Yamamoto, & Aiba, 1997; Arvanitoyannis, Nakayama, & Aiba, 1998; Arvanitoyannis, 1999), wound healing (Arvanitoyannis, Nakayama, & Aiba, 1998; Lloyd Kennedy, Methacanon, Paterson, & Jia & Shen, 1998), and a drug delivery system (Nunthanid *et al.*, 2004; Puttipipatkhachorn, Nunthanid, Yamamoto, & Peck, 2001). The use of chitosan in the application of drug delivery systems has received special interest. As a biocompatible, non-toxic, and hydrogel-like material, chitosan is a medically suitable candidate as a drug carrier for various drug types. It has been shown (Nunthanid *et al.*, 2004; Puttipipatkhachorn *et al.*, 2001) that the drug release behavior of chitosan is governed mainly by the swelling property, the dissolution characteristic of the polymer films, the pK_a of the drug, and the drug-polymer interaction.

In the present work, polyaniline/chitosan blend films were prepared and mechanical and electrical properties were investigated in terms of blend composition and the doping conditions: acid type, acid concentration, and doping time.

2. Experimental details

2.1. Materials

Chitosan (%DD = 80, M_v = 930,000) was prepared from shrimp shells (*Penaeus merguiensis*), kindly supplied by Surapon Food Public Co. Ltd, Thailand. Sodium hydroxide (50% w/w) solution was obtained from KPT Cooperation, Thailand. Glacial acetic acid (99.9% w/w, analytical grade) was purchased from J.T. Baker. Glutaraldehyde (50% w/w, analytical grade) was purchased from Fluka.

Aniline monomer was purchased from Merck Co. and was distilled under reduced pressure prior to use. Ammonium peroxodisulfate of AR grade was purchased from Merck Co. AR grade chemicals of *N*-methyl-2-pyrrolidone (NMP), hydrochloric acid, acetic acid, ammonia solution, and methanol were used as received.

2.2. Preparation of chitosan

Shrimp shells were cleaned and dried under sunlight before grinding into small pieces. The shrimp shell chips were then immersed in 1 M HCl for 2 days with occasional stirring. The product was washed with distilled water until becoming neutral and then soaked in a 4 wt% NaOH solution at 80–90 °C for 4 h. After the NaOH solution was decanted, the chips were washed again with distilled water until they became neutral, and then heated with 50 wt% NaOH solution in an autoclave at 110 °C for 1 h. The chitosan product was washed with distilled water until becoming neutral, and dried in an oven at 60 °C for 24 h.

2.3. Synthesis of polyaniline

The PANI in emeraldine base form (EB form) was prepared according to the method described by Cao, Andreatta, Heeger, and Stassen et al. (1989). In a typical procedure, 20.4 g of freshly distilled aniline monomer was dissolved in 230 ml of 1.5 M HCl and the solution was cooled to below 5 °C. A pre-cooled solution, at a temperature below 5 °C, containing 25 g $NH_4(S_2O_8)$ in 250 ml of 1.5 M HCl was slowly poured into the monomer solution for 1 h with vigorous stirring. The reaction temperature was maintained at 0–5 °C for 4 h. A dark green precipitate was recovered from the reaction mixture by filtering under reduced pressure and then washed thoroughly with a mixture of distilled water and methanol at the ratio of 80:20 (water–methanol) until the washing liquid was completely colorless and neutral. The precipitated product was treated with 300 ml of 3% ammonia solution at room temperature for 2 h. Upon filtering, washing with distilled water, and drying under dynamic vacuum at ambient temperature for 48 h, the blue powder of PANI in emeraldine base form was obtained.

2.4. Preparation of polyaniline/chitosan blend films

The emeraldine base form of PANI was dissolved in *N*-methyl-2-pyrrolidone (NMP) to obtain a 1 wt% solution. A 2 wt% solution of chitosan was obtained by dissolving chitosan in 2% acetic acid with vigorous stirring. 0.01 mole% of glutaraldehyde, as the crosslinking agent, was added into the chitosan solution. Depending on the desired fraction of PANI in the final mixture, an appropriate amount of PANI/NMP solution was mixed with a 2 wt% solution of chitosan. This mixture was stirred for 12 h at 25 °C. The resulting solution was cast onto a stainless steel mold and dried at 55 °C for 12 h. Finally, the films were removed from the molds and stored in desiccators prior to use.

2.5. Doping of polyaniline/chitosan composite films

The PANI/chitosan blend films were doped with aqueous HCl solutions of different concentrations and using various doping times. Subsequently, the films were placed between two sheets of filter paper and dried under vacuum at 25 °C for 48 h.

2.6. Characterization

The UV–Visible spectrum of synthesized PANI in the wave length range 200–800 nm was obtained using a Shimadzu UV–VIS spectrometer, model 2550. The light source was a deuterium lamp. *N*-Methyl-2-pyrrolidone was used as the solvent to prepare the polyaniline solution sample at the concentration of 0.3 g/l.

The FTIR spectra of PANI, chitosan, and the blend samples were recorded using a Thermo Nicolet Nexus 670 FTIR spectrometer in the absorbance mode at 32 scans with a resolution of 4 cm^{-1}. Spectra of frequency range of 4000–

400 cm^{-1} were measured using a deuterated triglycerinesulfate detector (DTGS) with specific detectivity of 1×10^9 cm $Hz^{1/2}$ w^{-1}.

The surface morphology of chitosan and the blend films was investigated using a scanning electron microscope (JOEL, model JSM-5800LV) at 10 kV with gold coating on the samples. The cross-sectional fracture surfaces of the blend films were obtained by cooling in liquid nitrogen followed by breaking.

Differential scanning calorimetry (DSC) of PANI, chitosan, and the blend samples was carried out in the temperature range 30–600 °C (Mettler-Toledo DSC 822) at a heating rate of 10 °C/min under a nitrogen atmosphere.

Thermogravimetric analysis (TGA) was used to evaluate the thermal stability and to determine the decomposition temperature of chitosan, PANI, and the blend films (Dupont Instrument TGA 5.1, model 2950). The temperature range studied was 30–600 °C at a heating rate of 10 °C/min under a nitrogen atmosphere.

The mechanical properties of PANI, chitosan, and blend films of different PANI contents were measured from dry rectangular film samples (10×1 cm) using a Universal Testing Machine (Lloyd, Model LRX) at 25 °C. A strain rate of 25 mm min^{-1} and gauge length of 50 mm was employed.

The electrical conductivity of chitosan, PANI, and the blend films was measured at 25 °C using a custom made two-point probe with an electrometer/high resistance meter (Keithley, model 7517A).

3. Results and discussion

3.1. UV–Vis spectra

UV–Vis spectroscopy was used to investigate the electronic state of the NMP-soluble fraction of synthesized PANI in EB form. The EB form of PANI shows two absorption peaks at 320 and 620 nm which can be assigned to the π–π* transition of the benzenoid ring and the exciton absorption of the quinoid ring, respectively (Cho *et al.*, 2004). The integral areas under these two peaks specify the concentration of the imine and the amine structure units as expected for the emeraldine oxidation state of PANI (Yang *et al.*, 2003).

3.2. FTIR spectra

FTIR spectra of PANI, chitosan, and PANI/chitosan blend films are shown in Fig. 1. For pure chitosan, the absorption peak at 3274 cm^{-1} is due to overlapping of the OH and NH_2 stretches (Nunthanid *et al.*, 2004). The peak appearing at 1716 cm^{-1} is due to the C=O stretch in $NHCOCH_3$ arising from a small portion of pristine chitin which was not deacetylated during the *N*-acetylation (Sung, Choi, & Jhon, 2002). The absorption peaks at 1548 and 1408 cm^{-1} can be assigned to the asymmetric and the symmetric stretching of carboxylate anions, indicating that chitosan molecules in the film were in the form of chitosonium acetate (Puttipipatkhachorn *et al.*, 2001). For the FTIR spectrum of pure PANI in the emeraldine base form, absorption peaks can be observed at 1567, 1493, 1305, and 828 cm^{-1} corresponding to the C=N stretching of the quinoid structure, the C–N stretching of the benzenoid structure, C–H stretching with the aromatic conjugation, and the vibration of symmetrically substituted benzene, respectively (Zhang & Wan, 2002).

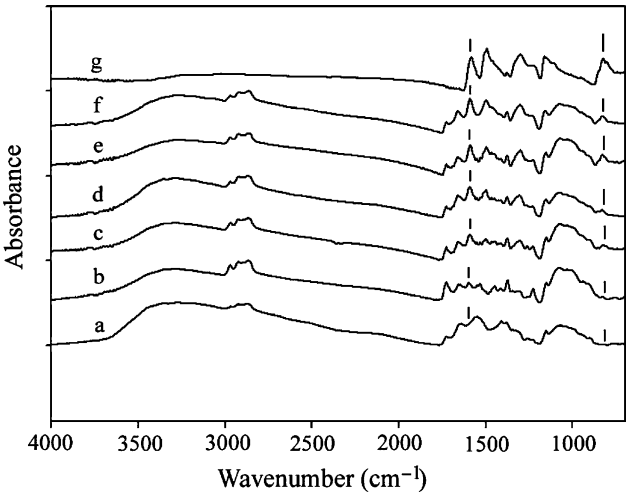

Fig. 1. FTIR spectra of PANI, chitosan, and PANI/chitosan blend films: (a) chitosan; (b) 10 wt% PANI; (c) 20 wt% PANI; (d) 30 wt% PANI; (e) 40 wt% PANI; (f) 50 wt% PANI; and (g) PANI.

These characteristic absorption peaks can also be observed in the FTIR spectra of chitosan/ PANI blends. As shown in Fig. 1, the characteristic absorption peaks of PANI become more dominant with increasing PANI content.

3.3. Morphology

SEM images of the surface morphology of pure chitosan and the blend films before and after treatment with NMP, used as the extraction solvent to remove PANI from the films, were investigated. Pure chitosan film showed a homogeneous surface and no characteristic change in morphology was observed after treatment with NMP. Chitosan did not dissolve in NMP therefore the original morphology was retained. On introducing 10 wt% PANI into the chitosan matrix, a smooth surface was still observed for the blend film. However, small holes were seen after extraction with NMP. This can be attributed to the removal of PANI particles from the surface of the film. On increasing the PANI content from 20–50 wt%, the films exibited rough surfaces and the roughness increased after treatment with NMP.

The visible characteristic of PANI/chitosan blend films was homogeneously of dark blue color, the color of pure polyaniline. The cross-sectional area surfaces of the blend films were investigated in order to study details of the dispersion of PANI in chitosan matrix. Fig. 2 shows SEM images of the cross-sectional fracture surface of the blend films. These micrographs clearly show that PANI particles

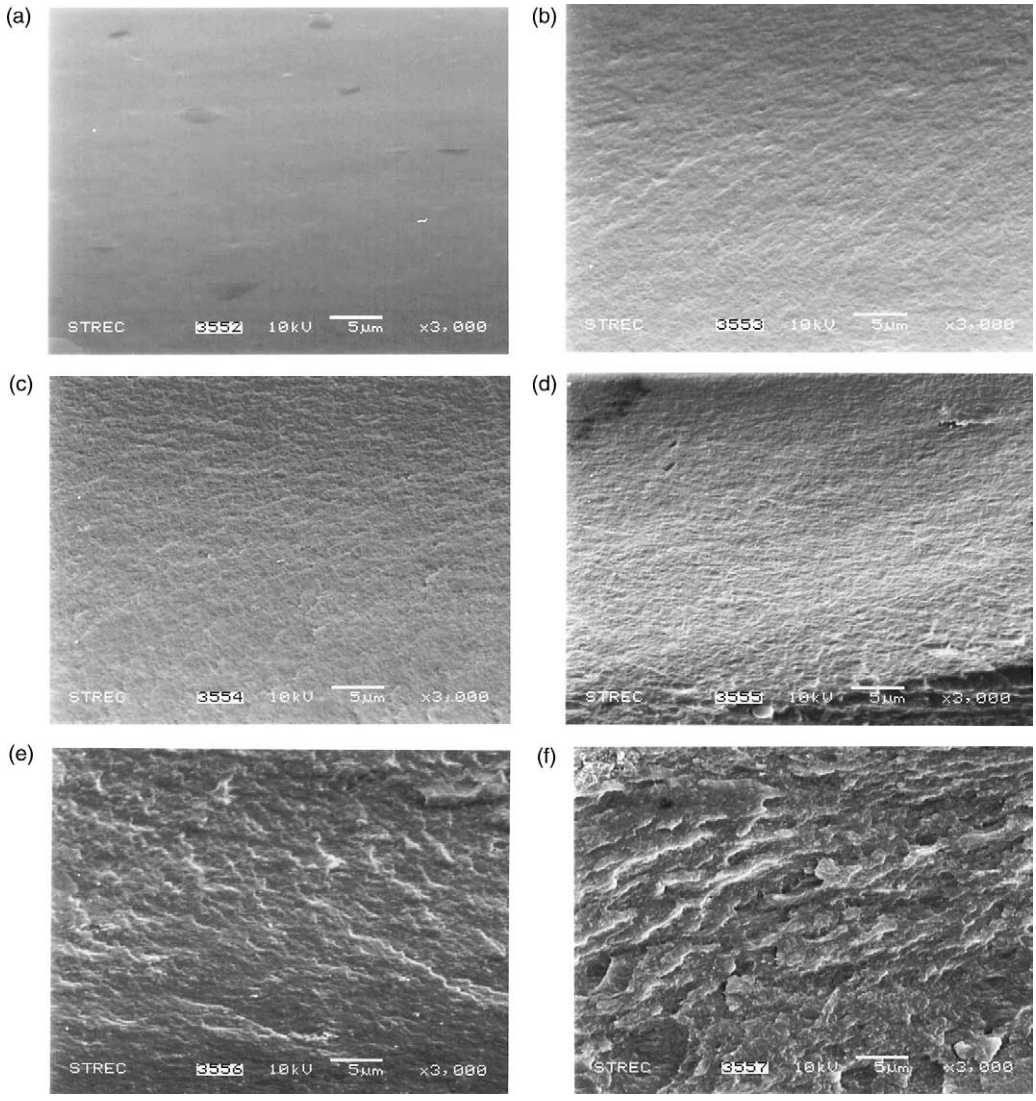

Fig. 2. SEM micrographs of the cross-sectional morphology of PANI/chitosan blend films: (a) chitosan; (b) 10 wt% PANI; (c) 20 wt% PANI; (d) 30 wt% PANI; (e) 40 wt% PANI; and (f) 50 wt% PANI.

were dispersed uniformly throughout the chitosan matrix when the content of PANI was lower than 50 wt% (Fig. 2a–e). Apparent voids or cracks can be seen in the blend with 50 wt% PANI (Fig. 2f), presumably due to the aggregation of PANI at this high PANI content. Our results can be compared with previous studies of PANI-β-NSA/PVA blend films (Zhang & Wan, 2002). The authors reported that PANI-β-NSA particles were dispersed uniformly in the PVA matrix when PANI-β-NSA content was lower than 12.6 wt% and distinct aggregates of PANI-β-NSA were observed when the content of PANI-β-NSA increased to 49 wt%.

3.4. Differential scanning calorimetry (DSC)

DSC thermograms of PANI, chitosan, and the blend films are shown in Fig. 3. The thermogram of pure PANI shows an

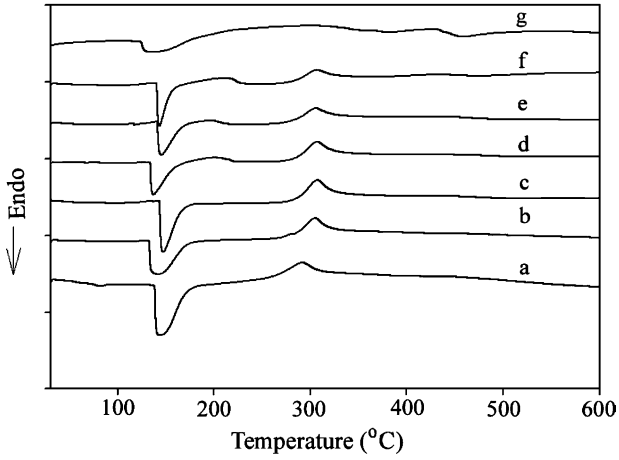

Fig. 3. DSC thermograms of PANI, chitosan, and PANI/chitosan blend films: (a) chitosan; (b) 10 wt% PANI; (c) 20 wt% PANI; (d) 30 wt% PANI; (e) 40 wt% PANI; (f) 50 wt% PANI; and (g) PANI.

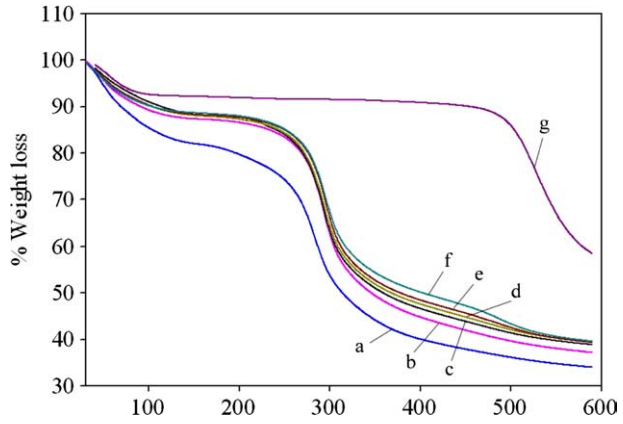

Fig. 4. TGA thermograms of undoped PANI, chitosan, and PANI/chitosan blend film: (a) chitosan; (b) 10 wt% PANI; (c) 20 wt% PANI; (d) 30 wt% PANI; (e) 40 wt% PANI; (f) 50 wt% PANI; and (g) PANI.

endothermic peak at around 120 °C owing to the evaporation of water. Broad exothermic peaks, observed between 200 and 400 °C, may be a result of interchain interaction between PANI chains. Another exothermic peak appears in pure PANI at 500 °C corresponding to the degradation of the PANI backbone (Gok, Sari, & Talu, 2004). In contrast, pure chitosan exhibits an endothermic peak at approximately 120 °C followed by an exothermic peak at 284 °C. These peaks indicate the loss of water and the degradation of chitosan, respectively (Kittur, Harish Prashanth, Udaya Sankar, & Tharanathan, 2001).

For the blend films, the degradation process took place at temperatures higher than for pure chitosan, indicating that the thermal stability of the blend films is higher than that of chitosan alone. Moreover, an exothermic peak at around 200 °C can be observed in the blend films containing 30–50 wt% of PANI. This suggests that the inter-chain interaction of PANI chains occurring with increasing PANI content.

3.5. Thermogravimetric Analysis

Fig. 4 shows the TGA thermogram of the PANI, chitosan, and their blend films. For pure PANI, two discrete weight losses occurred at approximately 100 and 500 °C corresponding to the loss of water and the degradation of PANI chains, respectively. In comparison, chitosan showed two discrete weight losses at approximately 100 and 284 °C reflecting the loss of water and the degradation of chitosan chains, respectively. Similar to chitosan, the blends containing 10–40 wt% PANI exhibit two weight loss steps due to the evaporation of water and the degradation of the blend. The degradation temperature (T_d) of the blend films increases with increasing PANI content, This result is consistent with the DSC result, which indicates that there was an intermolecular interaction, such as hydrogen bonding, between PANI and chitosan chains. In contrast, the blend film containing 50 wt% PANI exhibited two distinct degradation temperatures at approximately 295 and 500 °C, corresponding to the T_d of chitosan and PANI, respectively. This implies that a substantial phase separation was also present.

The TGA thermograms of PANI, chitosan, and the blends after doping with HCl solution are shown in Fig. 5. We see that the chitosan and blend films exhibited a lower T_d compared to those of the undoped films. This may be due to acid hydrolysis causing chitosan chain scission during the doping process.

3.6. Electrical property

Room temperature DC electrical conductivity values of PANI/chitosan blend films were measured before and after doping with various HCl concentrations, doping times, and different types of acid dopant. The doping sequence was

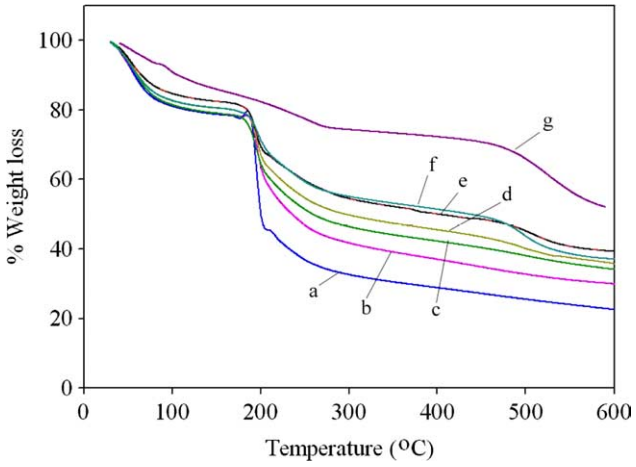

Fig. 5. TGA thermograms of PANI, chitosan, and PANI/chitosan blend film doped with 1 M HCl for 10 h: (a) chitosan; (b) 10 wt% PANI; (c) 20 wt% PANI; (d) 30 wt% PANI; (e) 40 wt% PANI; (f) 50 wt % PANI; and (g) PANI.

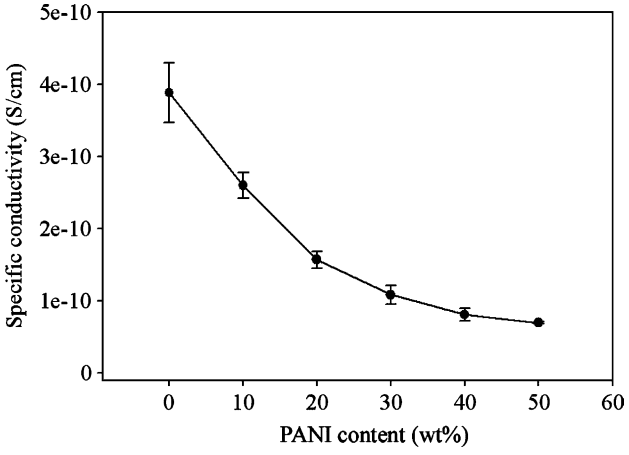

Fig. 6. The specific conductivity of undoped PANI/chitosan blend films as a function of PANI content.

Table 1
Specific conductivity and mechanical properties of the undoped and doped[a] PANI/chitosan blend films as a function of PANI content

PANI Content (%)	Specific conductivity (S/cm)		Young's modulus (MPa)		Tensile strength (MPa)		Elongation at break (%)	
	Before doping	After doping	Before doping	After doping	Before doping	After doping	Before doping	After doping
0	3.38×10^{-10}	7.56×10^{-8}	2912±570	2063±357	68.3±4.8	41.0±4.3	17.02±1.6	5.96±0.9
10	2.60×10^{-10}	7.69×10^{-7}	2828±296	1679±337	58.4±3.9	32.3±3.7	7.58±1.1	7.23±1.7
20	2.57×10^{-10}	2.15×10^{-5}	2970±360	2173±352	75.5±3.3	46.7±4.3	7.54±0.8	6.21±1.2
30	1.08×10^{-10}	4.27×10^{-5}	3212±242	2179±191	81.8±2.8	49.1±4.5	7.29±0.8	5.82±1.1
40	8.09×10^{-11}	1.23×10^{-4}	3138±504	2430±434	84.0±2.3	52.2±5.7	7.00±0.9	8.13±0.8
50	6.97×10^{-11}	4.16×10^{-4}	2689±386	2279±217	75.1±4.7	43.2±3.4	6.74±1.0	4.75±1.1
100[b]	4.09×10^{-11}	6.31×10^{-5}	–	–	–	–	–	–

[a] The blend films were doped with 0.5 M HCl for 2 h at 25 °C.
[b] The sample was prepared by compression of PANI powder.

visibly observed as the distinct color change from blue to green occurred.

3.6.1. Effect of blend composition

Fig. 6 shows the electrical conductivity of undoped PANI/chitosan blend films as a function of PANI content. The data, also tabulated in Table 1, indicate that the electrical conductivity of the blend films decreases with increasing PANI content. Pure chitosan has an appreciable conductivity, ca. 3.38×10^{-10} S/cm, due to the polarity of the protonated amino group of the chitosonium acetate. On addition of PANI EB, the insulating form of PANI, the ionic mobility of chitosonium acetate is disrupted, resulting in a decrease of electrical conductivity. On the other hand, after the blend films were doped with 0.5 M HCl for 2 h, the electrical conductivity of the blend films increased significantly with increasing PANI content, as shown in Fig. 7 and listed in Table 1. This is a direct result of the conversion of the emeraldine base form to the emeraldine salt form of a highly π-conjugated system. Finally, we noted that the blend films with PANI content higher than 50 wt% could not be fabricated due to excessive film brittleness.

3.6.2. Effect of hydrochloric concentration

The effect of HCl concentration on the electrical conductivity of the blend films at a 40 wt% PANI content was investigated and the data are shown in Fig. 8 and also tabulated in Table 2. The electrical conductivity of the films increases as the HCl concentration was increased from 0.1 to 1 M. The enhancement of the electrical conductivity with increasing HCl concentration is due to the increasing degree of protonation of the imine group of PANI. At higher HCl concentrations (2–6 M HCl), a decrease in electrical conductivity occurs. This result is probably due to over-protonation of PANI chains causing a decrease in the delocalization length of PANI.

3.6.3. Effect of doping time

Fig. 9 reveals that the electrical conductivity of the blend films varies with the doping time. The data are also tabulated in Table 3. The electrical conductivity of the blend films increases with increasing doping time from 0.5 to 10 h. Doping times longer than 10 h led to a decrease in electrical conductivity. This

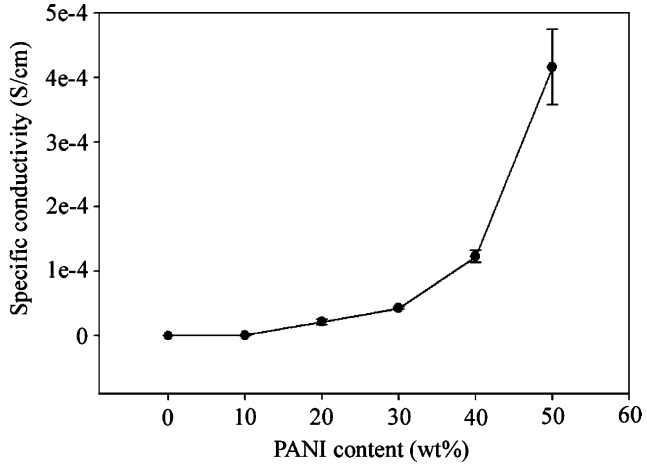

Fig. 7. The specific conductivity of doped PANI/chitosan blend films as a function of PANI content.

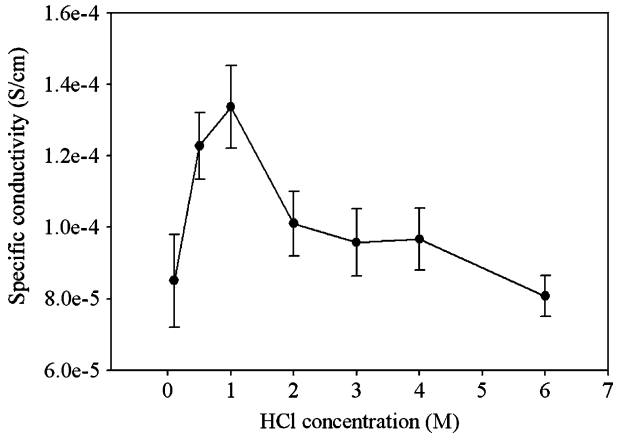

Fig. 8. The specific conductivity of doped PANI/chitosan blend films as a function of HCl concentration.

Table 2
Specific conductivity and mechanical properties of the undoped and doped[a] PANI/chitosan blend films as a function of HCl concentrations

HCl concentration	Specific conductivity (S/cm)		Young's modulus (MPa)		Tensile strength (MPa)		Elongation at break (%)	
	Before doping	After[a] doping	Before doping	After doping	Before doping	After doping	Before doping	After doping
0.1	8.09×10^{-11}	8.50×10^{-5}	3138±504	2434±316	84.0±2.3	53.2±3.0	7.00±0.9	11.35±1.5
0.5	8.09×10^{-11}	1.23×10^{-4}	3138±504	2430±434	84.0±2.3	52.2±5.7	7.00±0.9	8.13±0.8
1.0	8.09×10^{-11}	1.34×10^{-4}	3138±504	2149±310	84.0±2.3	51.5±4.0	7.00±0.9	7.58±1.1
2.0	8.09×10^{-11}	1.01×10^{-4}	3138±504	2160±164	84.0±2.3	49.4±3.8	7.00±0.9	6.82±1.1
3.0	8.09×10^{-11}	9.58×10^{-5}	3138±504	2199±209	84.0±2.3	49.2±3.8	7.00±0.9	6.08±0.9
4.0	8.09×10^{-11}	9.67×10^{-5}	3138±504	2022±229	84.0±2.3	48.5±5.4	7.00±0.9	6.29±0.9
6.0	8.09×10^{-11}	8.07×10^{-5}	3138±504	2101±238	84.0±2.3	46.3±4.5	7.00±0.9	4.10±0.9

[a] The blend films with 40 wt% PANI content were doped with HCl for 2 h at 25 °C.

is a result of the overprotonation of PANI occurring at prolonged doping times.

3.6.4. Effect of acid dopant type

Table 4 shows the electrical conductivity of blend films doped with different types of acid dopant. The nature of acid dopant, which involves a change in the strength and the size of the acid dopant molecule, evidently affects the electrical conductivity of the blend. The increase in electrical conductivity is due to a greater degree of protonation of the imine group of PANI as a result of a greater acid strength. The size of acid dopant also influences the electrical conductivity of blend films. The electrical conductivity decreases as the dopant anion size increases. Larger anions can more easily disrupt the orientation of PANI chains causing a lower degree of PANI chain packing. Hence, the electrical conductivity of the blend films decreases with increasing anion size.

3.7. Mechanical properties

The mechanical properties of the blend films at various blend compositions are tabulated in Table 1. Chitosan alone forms films with high values of tensile strength and modulus (68 and 2912 MPa, respectively). On addition of PANI, the Young's modulus of the blends essentially remains constant, within experimental error. However, the tensile strength decreases initially on addition of 10% PANI, presumably because the presence of PANI inclusions leads to weak points in the chitosan matrix. With further increase of PANI content from 20 to 40 wt%, however, tensile strength increases again. This may reflect a more uniform distribution of PANI in the chitosan matrix in which the particles shared loads. Upon introducing PANI in excess of 50 wt%, the blend became inhomogeneous, resulting in decrease in the tensile strength and the modulus. Table 1 also shows that the elongation at break decreases substantially on adding PANI, indicating that the blend films were more brittle than that of pure chitosan. Our observations appear to be consistent with previous studies on PANI/PVA blends (Gamgopadhyay & De, 2002; Mirmohseni & Wallace, 2003) which reported that a small amount of PANI (9 wt%) in the PVA matrix caused a decrease in tensile strength. On increasing the PANI content to 17 wt% the tensile strength increased due to a more uniform distribution of PANI in the PVA matrix, and the tensile strength decreased again after adding more PANI content. These results suggest that the processability of polyaniline can be improved by blending PANI with a soluble polymer as a matrix (Zhang & Wan, 2002).

After doping the blend films with HCl, Table 1 indicates that the tensile strength and the modulus decrease at all PANI compositions. Increases in HCl concentration and doping time cause decreases in the tensile strength and the modulus as shown in Tables 2 and 3, respectively. This result may be due to degradation of the chitosan network which acted as the matrix of the blend films (Jia & Shen, 2002; Varum, Ottoy, & Smidsrod, 2001) and also due to the well-known fact that PANI became more crystalline at higher doping levels. In addition to the effects of HCl concentration and doping time, the type of acid dopant can also affect the mechanical properties, as shown in Table 4. The mechanical properties dramatically decrease with higher strength of acid dopant because the higher acid strength

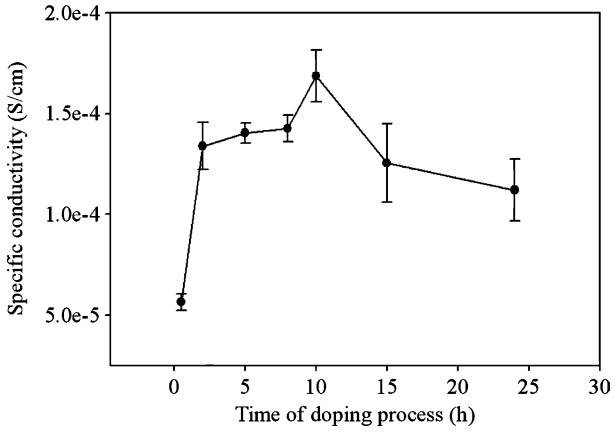

Fig. 9. The specific conductivity of doped PANI/chitosan blend films as a function of doping time.

Table 3
Specific conductivity and mechanical properties of the undoped and doped[a] PANI/chitosan blend films as a function of doping time

Doping time	Specific conductivity (S/cm)		Young's modulus (MPa)		Tensile strength (MPa)		Elongation at break (%)	
	Before doping	After doping	Before doping	After doping	Before doping	After doping	Before doping	After doping
0.5	8.09×10^{-11}	5.65×10^{-5}	3138±504	2236±262	84.0±2.3	53.0±4.2	7.00±0.9	5.92±0.5
2.0	8.09×10^{-11}	1.34×10^{-4}	3138±504	2149±310	84.0±2.3	51.5±4.0	7.00±0.9	7.58±1.1
5.0	8.09×10^{-11}	1.40×10^{-4}	3138±504	2055±296	84.0±2.3	50.6±4.3	7.00±0.9	6.69±0.9
8.0	8.09×10^{-11}	1.43×10^{-4}	3138±504	2067±251	84.0±2.3	49.2±4.1	7.00±0.9	6.26±0.5
10.0	8.09×10^{-11}	1.69×10^{-4}	3138±504	1948±260	84.0±2.3	48.5±4.0	7.00±0.9	6.54±0.9
15.0	8.09×10^{-11}	1.25×10^{-4}	3138±504	1881±264	84.0±2.3	42.4±3.9	7.00±0.9	7.00±1.2
24.0	8.09×10^{-11}	1.12×10^{-4}	3138±504	1708±346	84.0±2.3	41.4±3.6	7.00±0.9	8.31±1.7

[a] The blend films with 40 wt% PANI content were doped with 1 M HCl at 25 °C.

Table 4
Specific conductivity and mechanical properties of the undoped and doped[a] PANI/chitosan blend films as a function of type of acid dopant

Type of acid dopant	pK_a	Specific conductivity (S/cm)		Young's modulus (MPa)		Tensile strength (MPa)		Elongation at break (%)	
		Before doping	After doping	Before doping	After doping	Before doping	After doping	Before doping	After
Formic acid	3.75	8.09×10^{-11}	6.22×10^{-8}	3138±504	2234±355	84.0±2.3	60.7±5.7	7.00±0.9	13.71±1.7
Acetic acid	4.7	8.09×10^{-11}	2.01×10^{-8}	3138±504	2928±404	84.0±2.3	61.8±5.1	7.00±0.9	10.74±1.5
Ascorbic acid	4.2	8.09×10^{-11}	2.36×10^{-10}	3138±504	2762±471	84.0±2.3	75.2±4.1	7.00±0.9	6.11±1.0
Sulfuric acid	-3	8.09×10^{-11}	1.94×10^{-4}	3138±504	2574±251	84.0±2.3	48.3±4.1	7.00±0.9	7.15±1.3
Nitric acid	-1	8.09×10^{-11}	1.02×10^{-4}	3138±504	2475±260	84.0±2.3	51.7±3.7	7.00±0.9	8.06±0.9
Prechloric acid	-7	8.09×10^{-11}	4.07×10^{-5}	3138±504	2267±396	84.0±2.3	40.8±5.6	7.00±0.9	7.20±1.8
Hydro-chloric-acid	-6.1	8.09×10^{-11}	1.34×10^{-4}	3138±504	1948±260	84.0±2.3	48.5±4.0	7.00±0.9	6.54±0.9
p-toluene-sulfonic acid	-2.8	8.09×10^{-11}	1.42×10^{-5}	3138±504	2497±414	84.0±2.3	47.29±4.2	7.00±0.9	7.05±1.0

[a] The blend films with 40 wt% PANI content were doped with 1 M of acid concentration for 10 h at 25 °C except the concentration of ascorbic acid was 0.1 M.

caused a higher degree of chitosan chain scission in the blend films.

4. Conclusion

PANI/chitosan blend films were successfully prepared by a solution casting method. Smooth, flexible, and mechanically robust blend films were obtained at PANI content lower than 50 wt%. To become electrically conductive, the undoped PANI was doped with HCl. The electrical conductivity of the doped films increases with increasing PANI content. However, high concentrations of HCl (2–6 M) and long doping times (15–24 h) led to a decrease in electrical conductivity. This result indicates the over-protonation of PANI chains in the blend films. Moreover, increasing strength and using smaller anions for acid dopant induced higher electrical conductivity values of the blend films. The mechanical properties of the blend films were strongly affected by the doping treatment with HCl. The inferior mechanical properties of the blend films after doping were presumed to be due to hydrolysis of chitosan chains.

Acknowledgements

This work is financially supported by Chulalongkorn University through Conductive and Electroactive Research Unit and a grant provided by the Rachadapisek Somphot Endowment Fund. The authors wish to thank Surapon Food Public Co. Ltd, Thailand and KPT Cooperation, Thailand for supplying the materials and essential chemicals for this work.

References

Arvanitoyannis, I. (1999). Totally and partially biodegradable polymer blends based on natural and synthetic macromolecules: Preparation and physical properties and potential as food packaging materials. *Journal of Macromolecular Science*, *C39*(2), 205–271.

Arvanitoyannis, I., Kulokuris, I., Nakayama, A., Yamamoto, N., & Aiba, S. (1997). Physico-chemical studied of chitosan–poly(vinyl alcohol) blends plasticized with sorbitol and sucrose. *Carbohydrate Polymers*, *34*, 9–19.

Arvanitoyannis, I., Nakayama, A., & Aiba, S. (1998). Chitosan and gelatine based edible films: State diagrams, mechanical and permeation properties. *Carbohydrate Polymers*, *37*, 371–382.

Brahim, S., Narinesingh, D., & Guiseppi-Elie, A. (2002). Bio-smart hydrogels: Co-joined molecular recognition and signal transduction in biosensor fabrication and drug delivery. *Biosensors and Bioelectronics*, *17*, 973–981.

Cao, Y., Andreatta, A., Heeger, A. J., & Smith, P. (1989). *Influence of chemical polymerization condition on the properties of poly aniline*. USA: Institute for Polymer and Organic Solids, University of California.

Chipara, M., Hui, D., Notingher, P. V., Chipara, M. D., Lau, K. T., Sankar, J., et al. (2003). On polyethylene–polyaniline composites. *Composites Part B: Engineering*, *34*, 637–645.

Cho, M. S., Park, S. Y., Hwang, J. Y., & Choi, H. J. (2004). Synthesis and electrical properties of polymer composites with polyaniline nanoparticles. *Materials Science and Engineering C*, *24*, 15–18.

Crini, G. (2005). Non-conventional low-cost adsorbents for dye removal: A review. *Bioresource Technology*.

Gamgopadhyay, R., De, A., & Ghosh, G. (2001). Polyaniline–poly(vinyl alcohol) conductive composite: Material with easy processability and novel application potential. *Synthetic Metals*, *123*, 21–31.

Gangopadhyay, R., & De, A. (2002). Conducting semi-IPN based on polyaniline and crosslinked poly(vinyl alcohol). *Synthetic Metals*, *132*, 21–28.

Gok, A., Sari, B., & Talu, M. (2004). Synthesis and characterization of conducting substituted polyanilines. *Synthetic Metals*, *142*, 41–48.

Gupta, R. K., & Singh, R. A. (2004). Electrical properties of junction between aluminium and poly(aniline)–poly(vinyl chloride) composite. *Material Chemistry and Physics*, *86*, 279–283.

Gupta, R. K., Singh, R. A., & Dubey, S. S. (2004). Removal of mercury ions from aqueous solutions by composite of polyaniline with polystyrene. *Separation and Purification Technology*, *38*, 225–232.

Jia, Z., & Shen, D. (2002). Effect of reaction temperature and reaction time on the preparation of low-molecular-weight chitosan using phosphoric acid. *Carbohydrate Polymers*, *49*, 393–396.

Kim, B. C., Spinks, G., Too, C. O., Wallace, G. G., & Bae, Y. H. (2000). Preparation and characterization of processable conducting polymer–hydrogel composites. *Reactive and Functional Polymers*, *44*, 31–40.

Kittur, F. S., Harish Prashanth, K. V., Udaya Sankar, K., & Tharanathan, R. N. (2001). Characterization of chitin, chitosan and their derivatives by differential scanning calorimetry. *Carbohydrate Polymers*, *49*, 185–193.

Lima Pacheco, A. P., Araujo, E. S., & de Azevedo, W. M. (2003). Polyaniline/poly acid acrylic thin film composites: A new gamma radiation detector. *Materials Characterization*, *50*, 245–248.

Lloyd, L. L., Kennedy, J. F., Methacanon, P., Paterson, M., & Knill, C. J. (1998). Carbohydrate polymers as wound management aids. *Carbohydrate Polymers*, *37*, 315–322.

Mirmohseni, A., & Wallace, G. G. (2003). Preparation and characterization of processable electroactive polyaniline–polyvinyl alcohol composite. *Journal of Polymer*, *44*, 3523–3528.

Nunthanid, J., Laungtana-anan, M., Sriamornsak, P, Limmatvapirat, S, Puttipipatkhachorn, S, Lim, L.Y, et al. (2004). Characterization of chitosan acetate as a binder for sustained release tablets. *Journal of Controlled Release*, *99*, 15–26.

Puttipipatkhachorn, S., Nunthanid, J., Yamamoto, K., & Peck, G. E. (2001). Drug physical state and drug–polymer interaction on drug release from chitosan matrix films. *Journal of Controlled Release*, *75*, 143–153.

Small, C. J., Too, C. O., & Wallace, G. G. (1997). Responsive conducting polymer–hydrogel composites. *Polymer Gels and Networks*, *5*, 251–265.

Sung, J. H., Choi, H. J., & Jhon, M. S. (2002). Electrorheological response of biocompatible chitosan particles in corn oil. *Materials Chemistry and Physics*, *77*, 778–783.

Varum, K. M., Ottoy, M. H., & Smidsrod, O. (2001). Acid hydrolysis of chitosans. *Carbohydrate Polymers*, *46*, 89–98.

Won, W., Feng, X., & Lawless, D. (2002). Pervaporation with chitosan membranes: Separation of dimethyl carbonate/methanol/water mixtures. *Journal of Membrane Science*, *209*, 493–508.

Yang, X., Zhao, T., Yu, Y., & Wei, Y. (2004). Synthesis of conductive polyaniline/epoxy resin composites: Doping of the interpenetrating network. *Synthetic Metals*, *142*, 57-61.

Zhang, Z., & Wan, M. (2002). Composite films of nanostructured polyaniline with poly(vinyl alcohol). *Synthetic Metals*, *128*, 83–89.